ELSEVIER

Chemical Engineering Journal 136 (2008) 256–266

Chemical Engineering Journal

www.elsevier.com/locate/cej

Bioethanol steam reforming for ecological syngas and electricity production using a fuel cell SOFC system

Luis E. Arteaga [a,c,*], Luis M. Peralta [b], Viatshelav Kafarov [c], Yannay Casas [b], Erenio Gonzales [a]

[a] *Centro de Análisis de Procesos, Universidad Central de Las Villas (UCLV), Carretera a Camajuaní Km 5 y 1/2, Santa Clara, c/p 54830 Villa Clara, Cuba*

[b] *Departamento de Ingeniería Química, Universidad Central de Las Villas, Carretera a Camajuaní Km 5 y 1/2, Santa Clara, c/p 54830 Villa Clara, Cuba*

[c] *Universidad Industrial de Santander, Bucaramanga, Colombia*

Received 6 December 2006; received in revised form 16 March 2007; accepted 21 March 2007

Abstract

A bioethanol processing system to feed a 200 kW solid oxide fuel cell (SOFC) is simulated and evaluated in the present paper. The general scheme of the process is composed of vaporization, heating, bioethanol steam reforming (ESR) and SOFC stages. The performance pseudo-homogeneous model of the reactor, consisting of the catalytic ESR using a Ni/Al_2O_3 catalyst, has been developed based on the principles of classical kinetics and thermodynamics through a complex reaction scheme and a Lagmuir-Hishelwood kinetic pattern. The resulting model is employed to evaluate the effect of several design and operation parameters on the process (tube diameter between 3.81 and 7.62 cm, catalyst pellets diameter 0.1–0.5 cm, temperature 673–873 K, space time (θ) 1–10 (g min/cm^3) and water/ethanol molar ratio (R_{AE}), 1–6). It can be concluded that higher water/ethanol ratio (R_{AE} = 5:1) and temperatures (above 773 K) favors hydrogen yield (Y_H = 4.1) and selectivity (S_H = 91%), while the heat consumed in vaporization and heating stages is strongly increased at the same conditions. At temperatures above 773 K and $R_{AE} > 6$, the reforming efficiencies exhibit a plateau because of the thermodynamics constraints of the process. The SOFC stack is arranged in parallel and needs 83 cells of 0.4 A/cm^2 and 1 m^2.
© 2007 Elsevier B.V. All rights reserved.

Keywords: Bioethanol; Steam reforming; Fuel cells; Reactor modeling

1. Introduction

Nowadays catalytic steam reforming is a new interest focus as the main pathway to obtain hydrogen from hydrocarbons or alcohols to be supplied to a fuel cell (FC). The mentioned above is based fundamentally on the low emissions and high efficiency levels obtained from the operation of FC systems and hydrogen combustion engines as well [1–3]. The environmental compatibility of hydrogen energy is limited by the primary fuel, because of this ethanol present several advantages when is compared with other fuels [1], since it is easier to store, handle and transport in a safe way due to its lower toxicity and volatility. In addition, this alcohol could be bio-produced from a wide variety of biomass sources, including sugar cane molasses, lignocelluloses and waste materials from agro-industries [4]. On the other hand, if the fermentation of biomass is used to obtain the bioethanol, the total emissions of CO_2 could be neutral, since the dioxide emitted in the reforming to FC process is consumed for biomass growth, being the contribution to the total warming null.

Moreover, bioethanol steam reforming is the cheapest and efficient way to produce hydrogen from biomass, both reactants (water and ethanol) includes H atoms that contribute to the total yield and the thermal efficiency obtained is considerably good (>85%) [2]. From thermodynamic studies [5,6], the feasibility of hydrogen production from bioethanol steam reforming at temperatures higher than 500 K have been proved. Besides these studies has shown that the increment of temperature and water/ethanol feed molar ratio (R_{AE}) favors the hydrogen production while high pressures reduces considerably the total yield.

* Corresponding author.
E-mail address: luiseap@gmail.com (L.E. Arteaga).

1385-8947/$ – see front matter © 2007 Elsevier B.V. All rights reserved.
doi:10.1016/j.cej.2007.03.047

Nomenclature

A_{is}	shell inner transfer area (cm^2)
A_{os}	shell exterior heat transfer area (cm^2)
A_{refm}	mean area of heat transfer surface of refractory (cm^2)
A_s	shell flow area (cm^2)
A_{sm}	mean area of heat transfer surface of shell (cm^2)
A_t	tube flow area (cm^2)
A_{wm}	mean area of heat transfer surface of metal (cm^2)
Ac	SOFC stack surface (cm^2)
ac	single cell surface (cm^2)
C_{pm}	reacting mixture heat capacity (J/g K)
C_{pg}	hot gasses heat capacity (J/g K)
$C_{E\text{-}Exp}$	experimental bioethanol conversion
$C_{E\text{-}Model}$	predicted bioethanol conversion
D_p	pellet diameter (cm)
D_{to}	tube outer diameter (cm)
D_s	shell inner diameter (cm)
DI	current density (A/cm^2)
F_j	molar flow of component j (mol/s)
F_{obj}	optimization function
G_g	hot gasses mass flow (g/s)
G_m	reacting mixture mass flow (g/s)
h_{cr}	convection–radiation coeff. between surface and surroundings (W/cm^2 K)
h_{is}	convection–radiation film coeff. between shell and tubes (W/cm^2 K)
h_i, h_o	heat transfer film coeff. for inside and outside of tubes surface (W/cm^2 K)
$\Delta H_{(i)}$	heat of reaction i (J/mol)
I	current (A)
K_{eff}	effective thermal conductivity (W/cm K)
K_m, K_i	thermal conductivity of mixture and component i (W/cm K)
K_{tref}	thermal conductivity of refractory (W/cm K)
K_{ti}	thermal conductivity of insulating (W/cm K)
K_w	thermal conductivity of metal (W/cm K)
M_i	molecular weight of component i (g/mol)
n	carbon atoms in the products (1 for CO, CO_2, CH_4 and 2 for C_2H_6)
$n(z,j)$	moles of component j at (z) position (mol/s) ($j=1$ C_2H_6O, $j=2$ CH_4, $j=3$ CO, $j=4$ H_2, $j=5$ CO_2, $j=6$ H_2O, $j=7$ C)
$n(O_2)_{CON}$	oxidant feed to SOFC (mol/s)
N_c	cells number
N_{tub}	tube number
p_E	C_2H_6O partial pressure (atm)
p_w	H_2O partial pressure (atm)
p_H	H_2 partial pressure (atm)
p_{ME}	CH_4 partial pressure (atm)
p_D	CO_2 partial pressure (atm)
p_M	CO partial pressure (atm)
P	total pressure (atm)
P_c	stack power (kW)
Qa	heat consumed in the conditioning (kJ/h)
Qr	heat consumed in the reforming (kJ/h)
Qv	heat consumed in the vaporization stage (kJ/h)
Qc	heat consumed in the heating stage (kJ/h)
$r(z,i)$	rate of reaction i at z position, $i=5, 6, \ldots, 10$ (mol/s cm^3)
Re	Reynolds number
R_{do}, R_{di}	dirt scale for outside and inside of tubes (cm^2 K/W)
$S_{j\text{-}Exp}$	experimental selectivity of component j
$S_{j\text{-}Model}$	predicted selectivity of component j
T_a	environment temperature
T_g	hot gasses temperature (K)
T_m	reacting mixture temperature (K)
T_{tw}	tube wall temperature (K)
U_t	overall heat transfer coefficient (tubes) (W/cm^2 K)
U_s	overall Heat transfer coefficient (shell) (W/cm^2 K)
V_c	single cell voltage (V)
x_{ref}	thickness of refractory material (cm)
x_{im}	thickness of insulating material (cm)
X_{sw}	thickness of shell (cm)
y_i	mol fraction of component i
$Y_{j\text{-}Exp}$	experimental yield of component j
$Y_{j\text{-}Model}$	predicted yield of component j
z	reactor length (cm)

Superscripts

in	enter to the reactor
out	living the reactor

Greeks letters

α	stoichiometric coefficient of component (j) within reaction (i)
ε	bed porosity
η_{ref}	reforming efficiency (%)
η_{cell}	cell efficiency (%)
ρ_m	reacting mixture density (g/cm^3)

The bioethanol steam reforming is an endothermic reaction, for this reason the necessary heat has to be supplied from an external source; it could be represented in the simplest case by the following stoichiometry equation:

$$C_2H_5OH + 3H_2O \Leftrightarrow 2CO_2 + 6H_2 \qquad \Delta H^\circ = +173.5\,\text{kJ mol}^{-1}$$

However, during the process a series of side reactions take place (ethanol dehydration and decomposition) producing byproducts (CH_3CHO, C_2H_4, CH_3COOH), which compete for hydrogen atoms causing the reduction of the global yield; because of this the use of stable and selective catalytic formulations is an important issue for the process development.

At this time, a wide range of catalytic materials has been investigated but the transition metals have a special interest because of their profitability and stability in the reforming processes [1]. A number of Ni-based catalysts supported on different oxides have been reported as very active and selective for the steam reforming of bioethanol, being demonstrated what the catalyst supports plays an important role; based on these in the present paper a Ni/Al_2O_3 formulation is used, because of the stability, selectivity and cheapness reported for this catalyst [7–11].

Although many papers reports the performance of this catalyst in the E-S-R there are a little information referred to the general kinetic pattern and reaction mechanism involving this reaction scheme. In this sense Therdthianwong et al. [11] deduced a power law equation, Eqs. (1) and (2) fitted to an experimental data obtained on a commercial catalyst (Ni/Al_2O_3) and valid for 1 atm and 673 K:

$$r_1 = k_{ap} p_E^{2.5} p_A^9 \quad (1)$$

$$k_{ap} = 280,075 \quad (2)$$

where p_E and p_A are the partial pressures of ethanol and water, respectively (atm) and k_{ap} is the reaction constant (mol/g cat h $atm^{9.52}$).

The use of a similar catalyst for the crude bioethanol steam reforming was recently analyzed by Akande et al. [12], in this case the kinetic pattern was adjusted according to an Eley-Rideal mechanism being the controlling step the reaction between the adsorbed bioethanol molecules and the steam at the bulk gas, Eq. (4). The same paper reported another model based in a power law type equation Eq. (3), however, both expressions are adjusted supposing that the reaction takes place according to a simple step.

$$r_2 = 3.12 \times 10^{-2} e^{[-7560/RT]} N_A^{0.43} \quad (3)$$

$$r_3 = \frac{2.08 \times 10^3 \, e^{[-4430/RT]} N_A}{\left[1 + 3.83 \times 10^7 N_A\right]^2} \quad (4)$$

where N_A represent the bioethanol molar flow (kmol/s) and $r_{2,3}$ are the reaction rate (kmol/kg_{cat} s).

Although these equations have a great practice sense, their use to develop robust models that allow to analyze thoroughly the process are restricted, because of this in the present work a system of equations able to describe the kinetic mechanism are proposed. The mathematical complexity of the deduced kinetic expressions does not affect its practice character and due to this the developed models are used to obtain a new bioethanol steam reformer prototype, using the analogy between tubes and shell heat exchangers and fixed bed multitube reactors.

The solid oxide fuel cells are very suitable to be feed with syngas at high operating temperatures (>500 °C) and their use has various advantages in reference to a traditional generation systems and to others types of fuel cells, mainly: high efficiency in energy conversion, modularity, environmental compatibility, support reforming and water gas reaction, and the absence of noble materials as construction components. In the present paper, the general characteristics of a planar solid oxide fuel cells system are depicted mainly: cells arrangement, cells account and the fuel use to produce 200 kW of power and using a syngas produced in a bioethanol steam reforming plant.

2. Bioethanol steam reforming (E-S-R) reaction pathway

The reaction pathway that describes the E-S-R has been broadly discussed by several authors; however, all of them confirm a strong dependence between this pattern, the operational conditions, the composition of the catalyst and the redox characteristic of the support material. In the present paper the approaches reported by Comas et al. [4], are used, and a new reaction pattern is proposed (Eqs. (5)–(10)), which includes water gas shift reaction (WGSR), Eq. (6), complete methane steam reforming, Eq. (8) and coke production and conversion, Eqs. (9) and (10). In this way, the mass balance was closed according to the experimental data.

$$CH_3CH_2OH \rightarrow CH_4 + CO + H_2 \quad (5)$$

$$CO + H_2O \rightarrow CO_2 + H_2 \quad (6)$$

$$CH_4 + H_2O \rightarrow CO + 3H_2 \quad (7)$$

$$CH_4 + 2H_2O \rightarrow CO_2 + 4H_2 \quad (8)$$

$$2CO \rightarrow C + CO_2 \quad (9)$$

$$C + H_2O \rightarrow CO + H_2 \quad (10)$$

3. Bioethanol steam reforming. kinetic modeling

In the present work, the kinetic modeling of H_2 production by the steam reforming of pure ethanol using Ni/Al_2O_3 catalyst is performed. The overall objective is to obtain a kinetic model to describe the intrinsic rate of the reactions represented by Eqs. (5)–(10) using methods of simulation–optimization analysis. The derivation of these rate expressions is based on the mechanistic description of the all reaction steps together with empiric deductions and the reactor modeling by means of the isothermal plug flow approach. The results of these derivations, measurements and analyses are presented and discussed bellow.

3.1. Experimental conditions

The experiments were carried out by Comas et al. [4] in a conventional fixed bed reactor operated isothermally at atmospheric pressure. Employing the catalyst in the appropriate average size range (below 0.045 cm), appropriate feed space velocity and residence time (10^{-3} g min/cm^3) as well as other conditions necessary and required for plug flow and isothermal behavior in the reactor. Other criteria for packed-bed reactors were revised too; to ensure that flow conditions in the reactor were close to plug flow in order to eliminate back mixing and minimize channeling. These were: (a) ratio of catalyst bed height to catalyst particle size (L/D_p) > 50 and (b) ratio of internal diameter of the reactor to the catalyst particle size (D/D_p) > 10.

3.2. Estimation of the parameters of the rate models

The methodology used to obtain the reaction constants and the exponents of all species for the six kinetic expressions corresponding with Eqs. (5)–(10) and according to the experimental data reported by Comas et al. [4] is represented in Fig. 1. The followed procedure to fit the models was performed using as convergence criterion the final values of selectivity and yield (Eqs. (11)–(14); see Klouz et al. [13]).

$$S_j = \frac{F_j}{(F^{\text{in}}_{\text{CH}_3\text{CH}_2\text{OH}} - F^{\text{out}}_{\text{CH}_3\text{CH}_2\text{OH}})n} \tag{11}$$

$$S_{\text{H}} = \frac{F_{\text{H}}}{[3(F^{\text{in}}_{\text{ethanol}} - F^{\text{out}}_{\text{ethanol}}) + (F^{\text{in}}_{\text{water}} - F^{\text{out}}_{\text{water}})]} \tag{12}$$

$$C_{\text{E}} = \frac{F^{\text{in}}_{\text{ethanol}} - F^{\text{out}}_{\text{ethanol}}}{F^{\text{in}}_{\text{ethanol}}} \tag{13}$$

$$Y_j = \frac{F_j}{F^{\text{in}}_{\text{ethanol}}} \tag{14}$$

Using this procedure, several kinetic equations were proven and integrated responding to different reaction rate-determining steps, i.e. (ethanol decomposition over Ni sites (single site mechanism), reaction between adsorbed water molecules and adsorbed CH_4, CO (dual site mechanism), etc., . . .). Also some factors that do not represent any mechanistic theory were incorporated too, i.e. (ethanol exponent).

3.3. Mathematical procedure

The parameters within mechanism based rate equations and empiric rate models were determined using the plug flow model applied to an isothermal laboratory reactor described in Comas et al. [4]. A Runghe-Kutta fourth method was used to integrate the mass balance equations (DAE system) and an integral opti-

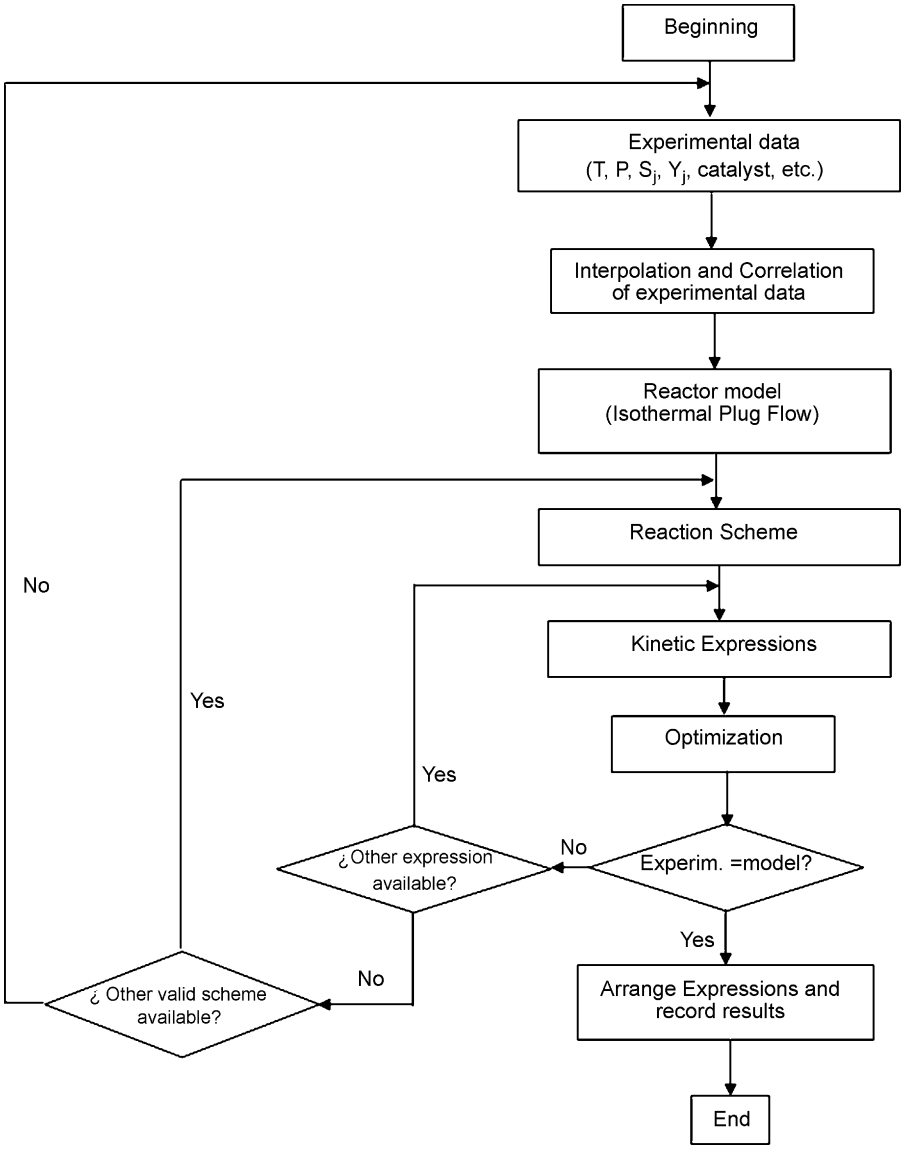

Fig. 1. Methodology used to obtain the kinetic parameters for bioethanol steam reforming.

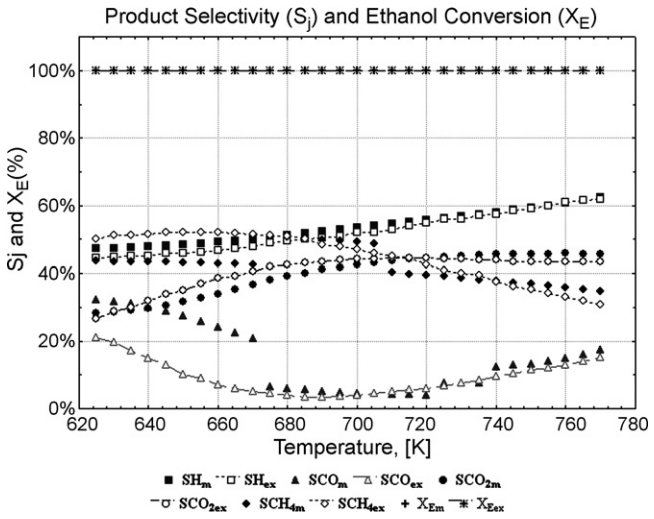

Fig. 2. Experimental vs. model predicted selectivity (S_j) and EtOH conversion (X_E) values at $R_{AE} = 3.3$.

mization subroutine coupled to a non-linear regression method (search of parameters-least squares) were used to obtain the optimum values that minimized the objective function represented by Eq. (15):

$$F_{obj} = \sum (S_{j-Model} - S_{j-Exp})^2 + \sum (C_{E-Model} - C_{Exp})^2 + \sum (Y_{j-Model} - Y_{j-exp})^2 \quad (15)$$

The exponents of each specie (n_j) and the rate constants (K_i) were changed and adjusted for temperatures between 673 and 873 K. The ethanol reaction exponent was varied in a wide range (0–5), and the best result was found at $n_{ethanol} = 1$, this exponent agrees with other authors reports, i.e. Sun et al. [2] found a first-order reaction with respect to ethanol (decomposition reaction). Moreover, Akande et al. [12] has shown an Eley-Rideal kinetic expression where the ethanol exponent is 1.

3.4. Results of the kinetic study

Fig. 2 represents the comparison of measured selectivity and predicted values using rate models and plug flow approach. The regression coefficients for all the compounds are very good for temperatures above the 673 K, the main statistic parameters of the samples were obtained using the software Statistica 6.0 and the results are depicted in Table 1 for the whole temperatures range. The model utilization at temperatures under the 673 K produces high departures from reality in CO and CH_4 selectivities. However, the deviations for H_2 and CO_2 are less drastic and the quality of the model in these cases is very good for the whole temperature range (see R^2 in Table 1). The kinetic expressions reported in Table 2 are those that best fit the experimental data.

Table 1
Model statistics

	Mean	S.D.	R^2
Experimental (S_j)			
Hydrogen	0.521	0.0564	–
Monoxide	0.0761	0.0385	–
Dioxide	0.405	0.053	–
Methane	0.4164	0.06652	–
Model (S_j)			
Hydrogen	0.536	0.0471	0.907
Monoxide	0.0851	0.0455	0.861
Dioxide	0.397	0.063	0.815
Methane	0.4194	0.06172	0.8931

Subscripts (ex) and (m) are referred to the experimental and the model values, respectively.

The R squared obtained for all the compounds are fairly good and allows to apply the model to solve design problems involving bioethanol steam reforming on Ni/Al_2O_3 catalyst. In the next sections, the design problem is solved step by step.

4. Steam reformer model equations

The fundamentals of fixed bed reactor (multi-tube and jacketed reactor) design exposed by Smith [14] are used to design the steam reforming reactor. The pseudo-homogeneous plug flow model is used to solve the mass, energy and momentum balances (Eqs. (16)–(19)) in the whole modeling environment:

- Mass balance

$$\frac{dn(z,j)}{dz} = A_t(1-\varepsilon)\sum_i \alpha(j,i) r(z,i) \quad (16)$$

- Energy balance

Table 2
Kinetic pattern of bioethanol steam reforming

Constants E_a (J/mol)	Expressions (mol/s cm^3)
$K_5 = 93.207\, e^{(-64597.4/RT)}$ (5)	$r_5 = K_5 \times \frac{p_E}{\alpha^2}$
$K_6 = 2.17 \times 10^{-7}\, e^{(-5110.81/RT)}$ (6)	$r_6 = \frac{K_2}{\alpha^2 \times p_H} \times \left(p_M p_w - \frac{p_D \times p_H}{K_e}\right)$
$K_7 = 1.06 \times 10^{28}\, e^{(-524{,}000/RT)}$ (7)	$r_7 = \frac{K_3}{\alpha^2 \times p_H^{2.5}} \times \left(p_{ME} p_w - \frac{p_M \times p_H^3}{K_e}\right)$
$K_8 = 8.01 \times 10^{-2}\, e^{(-83{,}810/RT)}$ (8)	$r_8 = \frac{K_4}{\alpha^2 \times p_H^{3.5}} \times \left(p_{ME} p_w^2 - \frac{p_D \times p_H^4}{K_e}\right)$
$K_9 = 4.625\, e^{(-41934.9/RT)}$ (9)	$r_9 = \frac{K_5}{\alpha^2} \times \left(p_M^2 - \frac{p_D}{K_e}\right)$
$K_{10} = 3.23\, e^{(-129{,}500/RT)}$ (10)	$r_{11} = \frac{K_6}{\alpha^2} \times \left(p_w - \frac{p_M \times p_H}{K_e}\right)$
$\alpha = 1 + K_{CO} \times P_M + K_{CH_4} \times P_{ME} + K_H \times P_H + \frac{K_{H_2O} \times p_w}{P_H}$	

Tube side:

$$\frac{dT_m(z)}{dz} = \frac{A_t}{G_m C_p}\left[\frac{4U_t}{D_{to}}(T_{tw}(z) - T_m(z)) - (1-\varepsilon)\sum_i \alpha(j,i) r(i)\,\Delta Hr(i)\right] \quad (17)$$

Shell side:

$$\frac{dT_g(z)}{dz} = \frac{A_s}{G_g C_p (D_s^2 - D_{to}^2)}[4U_t N_{tub} D_{to}(T_g(z) - T_m(z)) + 4U_s D_s (T_g(z) - T_a)] \quad (18)$$

- Pressure drop: modified Ergun equation [15].

$$\frac{dP(z)}{dz} = -\frac{G_m^2}{\rho_m A_t^2 D_p}\left(\frac{1-\varepsilon}{\varepsilon^3}\right) \times \left[1.75 + 4.2Re^{0.833}\frac{1-\varepsilon}{Re}\right]\frac{1}{1013250.1} \quad (19)$$

- Overall heat transfer coefficients:

Overall heat transfer coefficients for reactor tubes and shell are calculated considering a geometrical analogy between fixed bed multi-tube reactors and shell and tube heat exchangers. Eq. (20) from Perry and Green [16] and Eq. (21) from Peters et al. [17] are used to estimate these coefficients for the tubes and shell side, respectively.

$$U_t = \frac{1}{(1/h_o) + R_{do} + (x_{tw} A_{ot}/K_w A_{wm}) + ((1/h_i) + R_{di}) A_{ot}/A_t} \quad (20)$$

$$U_s = \frac{1}{(1/h_{cr}) + (x_{ref} A_{1s}/K_{tref} A_{refm}) + (x_{sw} A_{1c}/K_{ts} A_{wm}) + (x_{im} A_{1c}/K_{ti} A_{sm}) + ((1/h_{is}) + R_{do}) A_s/A_{os}} \quad (21)$$

All the individual heat transfer coefficients involving non-reacting systems (shell to tubes and from shell to surroundings) are determined by means of the equations reported by Perry and Green [16] Section 5 and 11. To calculate the heat transfer coefficient (h_i) from tubes wall to reforming gases is used the well known equation developed by Leva (Eq. (22)):

$$\frac{h_i D_t}{K_m} = 0.813\left(\frac{D_p G_m^{0.9}}{\mu_m}\right)\exp\left(\frac{-6D_p}{D_t}\right) \quad (22)$$

Thermal conductivity of the gas mixture and effective conductivity (gas/catalyst) are calculated by the following recommended method of averaging [14,15].

$$K_m = \frac{\sum y_i K_i (M_i)^{0.33}}{\sum y_i (M_i)^{0.33}};$$

$$K_{eff} = \frac{K_m}{D_t}\left(\frac{K_p}{K_m}\right)^{0.12}(1.036 + 0.00178Re) \times 10^{-2} \quad (23)$$

Viscosity of the gas mixtures is calculated in a similar manner:

$$\mu_m = \frac{\sum y_i \mu_i (M_i)^{0.5}}{\sum y_i (M_i)^{0.5}} \quad (24)$$

- Tube number

The tubes number is calculated by a simple optimization procedure using Eq. (25), this expression is deduced from the data exposed by Perry and Green [16] and restricted to:

$$\text{total pressure drop} : \frac{P_{in} - P_{out}}{P_{in}} \le 0.3$$

$$\text{ethanol conversion} : X_{ethanol} = 100\%$$

$$\text{hydrogen flow} : n_H \ge 2.159\ (\text{mol/s})$$

$$\text{constant parameter} : 20 < C_C < 26$$

$$N_{tub} = 1298 + 74.86C_C + 1.283C_C^2 - 0.0078C_C^3 - 0.0006C_C^4 \quad (25)$$

After defining the reformer model and before simulating the fuel cells calculations are performed because the design procedure is a feed-forward method between these two models.

5. Fuel cell calculations

There are many different ways to approach this problem, some of which may seem rather complex because of the simultaneous reactions (fuel cell, reforming and water gas shift reaction) and the recycle stream supplying moisture required for the reforming reaction. We shall simplify the solution to this problem, by focusing these three reactions by means of a mechanism in series and using basics of chemical reaction engineering. The hydrogen production by internal CH_4 reforming and WGSR is not considered to estimate the H_2 initial needs (Section 5.1).

5.1. Theoretical hydrogen needs

The quantity of hydrogen needed to produce 200 kW of power is calculated from the correlations of continuous current circuits and the Faraday's law applied to a fuel cells system, assuming a cell voltage of 0.6 V [3] and the efficiency concept (Eq. (26)):

$$\eta_{cell} = \frac{0.83V_c}{V_{ideal}} = \frac{0.83V_c}{1.229} = 0.675V_c = 40.5\% \quad (26)$$

where V_{ideal} is the cell ideal voltage (Hirschenhofer et al. [3]).

Then for a parallel arrangement:

$$I = \frac{P_C}{V_c} = \frac{200,000\ \text{W}}{0.6\ \text{V}} = 3.3 \times 10^5\ \text{A} \quad (27)$$

Therefore with this information and assuming a fuel utilization coefficient of 0.85, the necessary theoretical hydrogen ascends to:

$$F_H = 3.3 \times 10^5\,A \left(\frac{1\,C/s}{1\,A}\right)\left(\frac{1\,mole^{-1}}{96,487\,C}\right)\left(\frac{1\,mol\,H_2}{2\,mole^{-1}}\right) \times \left(\frac{3600\,s}{1\,h}\right)\left(\frac{1}{cuc}\right) = 2.159\,mol\,H_2/s$$

The quantity of ethanol to feed the reforming stage is determined using a feed-forward procedure between H_2 needs and the yield approach, Eq. (14).

5.2. Theoretical oxidant needs

To obtain the oxygen need in a fuel cells system the first step is look into the reaction stoichiometry between the O_2 and H_2. For a simple reaction:

$$2H_2 + O_2 \rightarrow 2H_2O$$

Assuming a utilization coefficient of 25%:

$$n(O_2)_{CON} = \frac{1\,mol\,O_2}{2\,mol\,H_2} \times 2.159\,mol\,H_2/s \times 4 = 4.32\,mol\,O_2/s$$

5.3. Number of cells

The number of cells is a direct function of the design power and the arrangement, being established:

5.3.1. Parallel arrangement

The fuel cell module voltage is the same as the cell voltage, and the fuel cell module current is equal to the current of an individual cell times the number of fuel cells.

5.3.2. Series arrangement

The fuel cell module voltage obey the same law that the current for a parallel array:

$$V_{stack} = V_{cell} \times \text{No. of cell.}$$

The data reported by Brandon et al. [18] is used to determine the module area for an operational temperature of (873 K) and 400 (mA/cm^2) of current density (DI).

$$Ac = \frac{I}{DI} = \frac{3.3 \times 10^5\,A}{0.40\,A/cm^2} = 8.25 \times 10^5\,cm^2$$

For a cell area of 1 m^2 the number of cells in parallel can be determined:

$$N_c = \frac{Ac}{ac} = \frac{8.25 \times 10^5\,cm^2}{10,000\,cm^2} = 83\,cells$$

5.4. Fuel cell reaction

Applying the basic principles of chemical engineering is possible to arrive to a preliminary result for the internal behavior of the fuel cells stack. Before proceeding with the fuel cell calculations, it is important to point out that the analysis is done assuming three fundamental reactions occurring inside the SOFC at 873 K:

$$CH_4 + 2H_2O \rightarrow CO_2 + 4H_2 \quad (28)$$

$$CO + H_2O \rightarrow CO_2 + H_2 \quad (29)$$

$$H_2 + 1/2O_2 \rightarrow H_2O \quad (30)$$

It is also assumed that these reactions respond to a series mechanism: methane steam reforming (Eq. (28)), water gas reaction (Eq. (29)) and hydrogen conversion (Eq. (30)). Equilibrium conditions for CO reaction are evaluated by means of the extent ($\times$) of the reaction:

6. Reactor simulation

The model equations discussed in the previous sections are used to simulate the reformer behavior at changes in design and operation variables. This procedure allows to obtain the reactor prototype that exhibit better performance at process conditions. The design alternatives considered are represented in Table 3.

6.1. Effect of space time and tube number

Ethanol conversion at all the evaluated residence times is 100% (see Table 2). The residence time increment (catalyst weight/vol. flow), guarantees the contact between reactants and catalyst causing the decrease in the molar flow of ethanol feed into the reactor and the increment in the hydrogen yield ($Y_H = 3.06$ at 0.01 g min/cm^3). The reactor operation is restricted by the pressure drop ($\Delta P > 30\% P_o$) when 100 tubes are used and an over design is evidenced for 200 tubes because the profits for bioethanol saving and H_2 production are too close to the others design alternatives (see Table 4). The use of 150 tubes guarantees the operation with yield levels (1.26–3.06) considerably good under the proposed operation conditions.

6.2. Effect of tube diameter

The internal distribution of the catalyst is favored by the increment in the tube diameter; it allows the work under permissible conditions of pressure drop and facilitates the heat exchange area to meet the heat requirements of the process. The evaluated alternatives for tube diameter (3.81–7.62 cm) in a bioethanol steam reformer exhibits a maximum region for hydrogen yield

Table 3
Design alternatives for bioethanol reformer

Parameter	Range	U/M
Tube inner diameter	3.81–7.62	cm
Pellet diameter	0.1–0.5	cm
Space time	0.001–0.01	g_{cat} min/cm^3
Water/ethanol ratio	3–6	–
Temperature	673–873	K
Tubes number	100–200	–

Table 4
Space time and number of tubes effect on ESR

θ (g min/cm^3)	N_{tub}	L_{react} (cm)	X_{ETOH} (%)	Y_H	N_{EO} (mol/s)
0.001		62	100	1.03	2.09
0.005	100	121	100	2.63	0.82
0.01		222	100	2.87	0.75
0.001		34	100	1.26	1.72
0.005	150	75	100	2.84	0.78
0.01		140	100	3.06	0.705
0.001		25	100	1.30	1.65
0.005	200	55	100	2.89	0.745
0.01		102	100	3.14	0.685

(5.08 cm); this is closely related with the thermodynamic characteristics of the reaction taking place, as shown by Laborde and Garcia [5] and Casas et al. [19] hydrogen yield suffers a fall with the pressure and is favored with temperature increase; because of these: the increase in the tube diameter could infer a decrease in the hydrogen yield due to the total pressure effects (small reductions), however, this fall is compensated with the increment of the heat transfer area which is a key parameter to supply the process energy requirements to complete the reforming reactions (methane reforming).

In Table 5 are represented the design parameters of the reactor prototype that has shown the best results for bioethanol steam reforming reaction.

After the exhaustive screening described above, it can be concluded that the combination among the space time, tube and particle diameter exposed in Table 5, conform the ideal reactor to be used for the ethanol steam reforming at the referred conditions, this conclusion is based in the yield indexes (3.06) and the pressure drop obtained along the reactor ($P_{out} < 0.3P_{in}$).

6.3. Effect of operational variables

The reactor model and the variables exposed in Table 5 are used to study the influence of the operational parameters (T and R_{AE}) on the analyzed process. The temperature and water to ethanol molar ratio feed into the reactor are the independent variables in the simulation strategy; these variables are identified as key parameters to obtain high levels of efficiency, by means of their influence on the chemical reaction and on the conditioning stages (vaporization-heating). Reactor internal profiles of temperature, pressure and concentration are obtained by means of the mentioned model and reported as well. The obtained results are exposed in Figs. 3–6.

Table 5
Design results to supply H_2 to a 200 kW SOFC

Parameter	Value	U/M
Space time	0.01	g_{cat} min/cm^3
Pellet diameter	0.1	cm
Tube inner diameter	5.08	cm
Tube number	150	–
Temperature	673–873	K
Water/ethanol ratio	3–6	–
Ethanol molar flow	1.07	mol/s

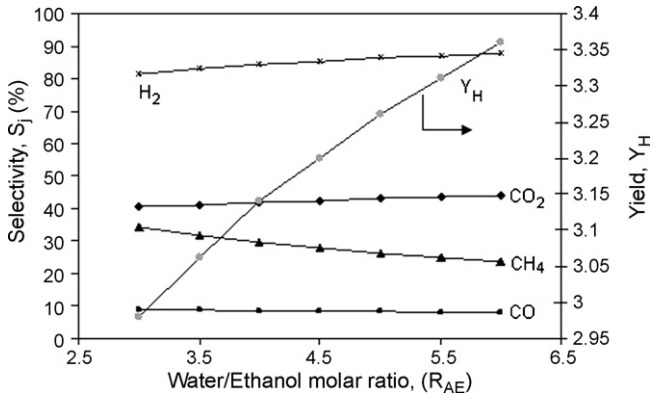

Fig. 3. Influence of water/ethanol molar ratio (R_{AE}) on products selectivity and hydrogen yield: $T = 773$ K and $\theta = 10^{-2}$ g min/cm^3.

Water/ethanol molar ratio at the reactor inlet and the reaction temperature, has a positive effect on hydrogen yield (4.1 at 873 K and $R_{AE} = 5$), that can be corroborated in Figs. 3, 4 and 6, this result agrees with Comas et al. [4] and Klouz et al. [13]. The impact of these variables could be attributed to the mass and kinetic effects, respectively, that is to say: an increment in the water/ethanol ratio cause a proportional effect in the quantity of H_2 available to be extracted (2 atoms per water molecule), considering that the main production of hydrogen comes from the methane steam reforming and WGSR, respectively, Eqs. (6)–(8).

The CH_4 selectivity is slightly decreased from 0.34 to 0.23 when R_{AE} varies from 3.3 to 6 while hydrogen production is strongly improved at the same conditions (Fig. 3), this means that molar ratios higher than 3.3 promotes CH_4 reforming and WGSR (this can be corroborated by means of the increase of CO_2 selectivity at the same conditions). Moreover, whatever amount of water initially feed into the reactor the ethanol conversion reached is 100% for the whole temperatures explored, that agrees completely with the results reported by Akande et al. [12] and Klouz et al. [13] under similar operational conditions. Also the reaction temperature favors the process considerably (Figs. 4 and 6) ($S_H = 91\%$ at 873 K) because the general process is highly endothermic and the kinetics of the CH_4 steam reforming is favored as well.

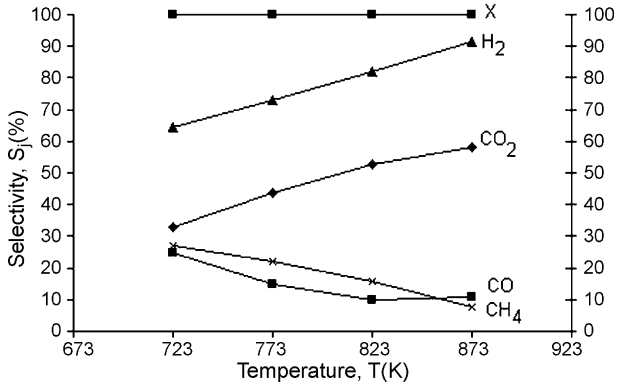

Fig. 4. Influence of temperature (T) on products selectivity and hydrogen yield: $R_{AE} = 5$ and $\theta = 10^{-2}$ g min/cm^3.

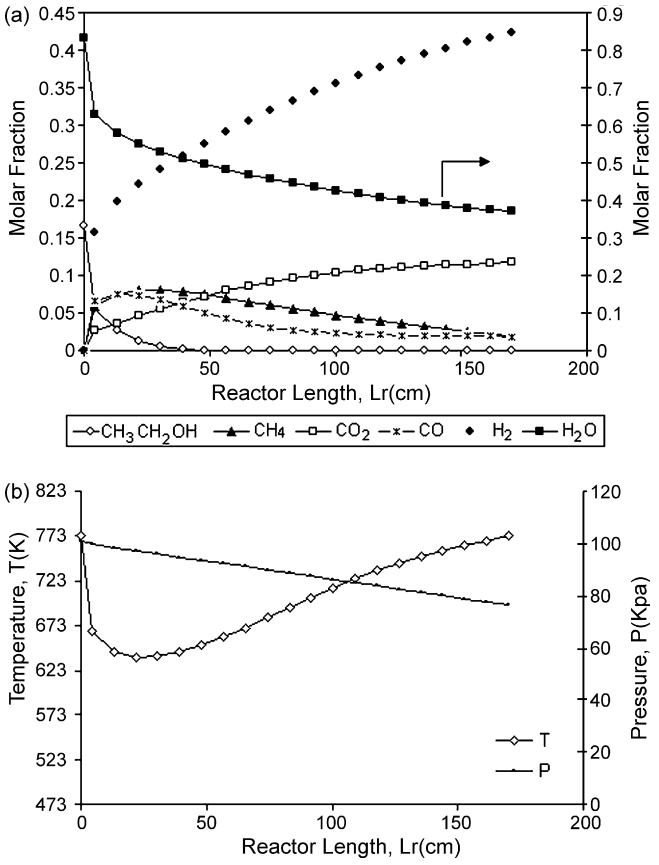

Fig. 5. (a) Reactor internal concentration profiles. $R_{AE} = 5$, $T = 773$ K and $\theta = 10^{-2}$ g min/cm^3. (b) Reactor internal temperature and pressure profiles. $R_{AE} = 5$, $T = 773$ K and $\theta = 10^{-2}$ g min/cm^3.

The developed model describes perfectly the series/parallel behavior of the proposed reaction pathway. If the reactor internal profiles are analyzed could be concluded that the model describes clearly the intermediate behavior reported previously by Comas et al. [4] and Klouz et al. [13] for CH_4 and CO and the profiles of the other species (H_2O, H_2 and CO_2) are consequent with the proposed reaction pathway.

7. Global plant simulation

The flow diagram (approximate) of the plant for syngas production using bioethanol coupled to the fuel cells system is represented in Fig. 7. The section of electric generation (fuel cell) is simplified to obtain a better picture of the system.

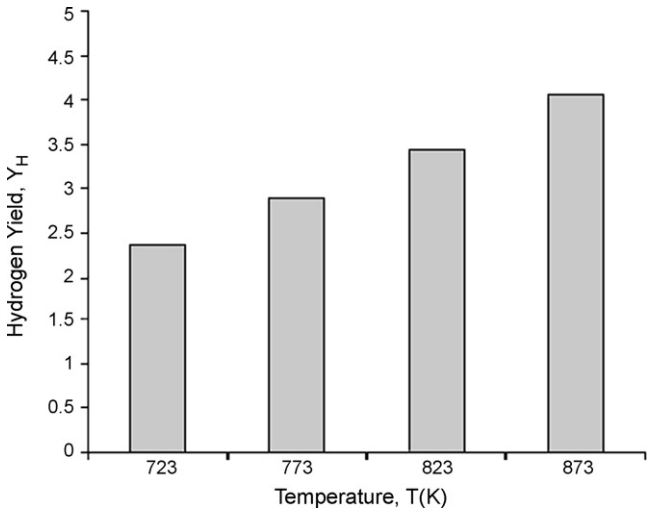

Fig. 6. Temperature influence on hydrogen yield: $R_{AE} = 5$ and $\theta = 10^{-2}$ g min/cm^3.

The effect of temperature and the water ethanol molar ratio on the performance of preparation, reforming and fuel cell stages is studied by means of simulation procedure and using an integrated system flow.

7.1. Effect of water/ethanol molar ratio

The influence of water/ethanol molar ratio on ethanol steam reforming process (vaporization + heating + reforming) follows the basic principles of thermodynamic and heat transfer: the change in the mixture composition (increment with the less volatile component) causes a direct increment of the boiling point and the total flow and these factors are directly proportional to the energy consumption (sensitive heat) in the heating, reforming and conditioning stages, respectively (see Fig. 8).

The water content of the reacting mixture has a relevant effect on the levels of hydrogen produced in the reforming stage (as was discussed above), on the changes in the energy capacity (LHV) of the synthesis gas and the cell exhaust. In the present paper, a novel criterion is used to determine the effect of the R_{AE} on the steam reforming reaction: efficiency (η_{RE}): is defined as

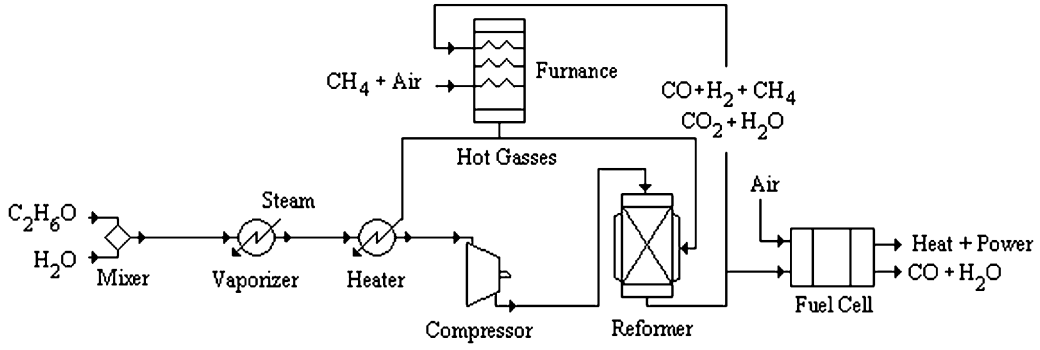

Fig. 7. Approximate flow diagram for the process.

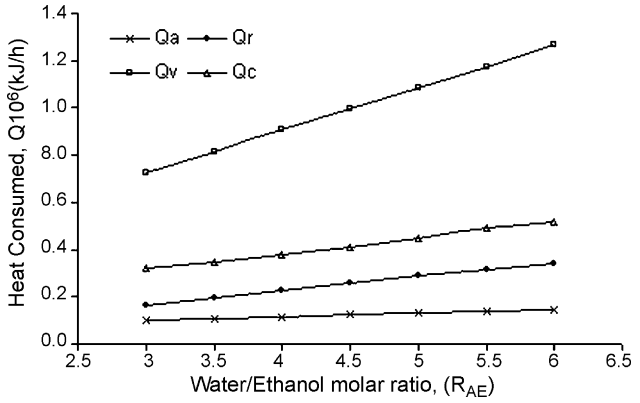

Fig. 8. Water/ethanol molar ratio influence on energy consumption: $T = 773$ K and $\theta = 10^{-2}$ g min/cm^3.

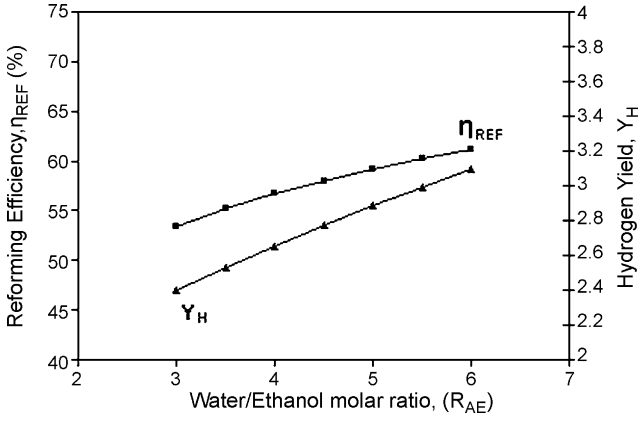

Fig. 9. Water/ethanol molar ratio influence on reforming efficiency and hydrogen yield: $T = 773$ K and $\theta = 10^{-2}$ g min/cm^3.

the ratio of the H_2 actual molar flow and the maximum molar flow obtained under equilibrium conditions.

The water/ethanol molar ratio favors the reforming efficiency (see Fig. 9). While R_{AE} increases from 3 to 6 the efficiency is favored (53–61), from this point forward the curve begins to form a plateau due to the process thermodynamic limitations, being expected that this tendency becomes worse for $R_{AE} > 8$ accordingly to that exposed by Diagne et al. [20]. The fuel cell exhibit an energy use of the synthesis gas of 85–95% (see Fig. 10).

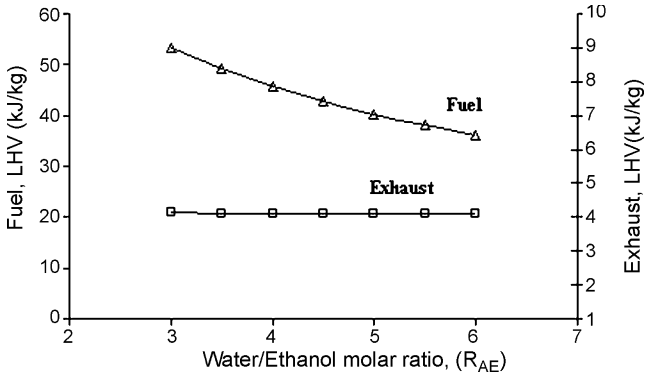

Fig. 10. Water/ethanol molar ratio influence on fuel and exhaust energy content: $T = 773$ K and $\theta = 10^{-2}$ g min/cm^3.

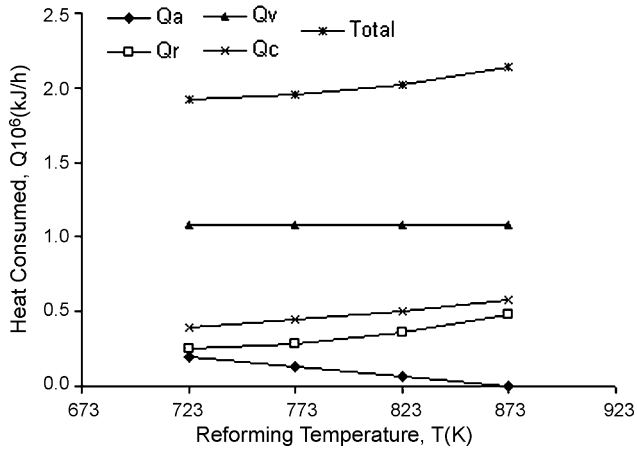

Fig. 11. Temperature effect on the heat consumed at all process stages: $R_{AE} = 5$, $T = 773$ K and $\theta = 10^{-2}$ g min/cm^3.

7.2. Effect of the temperature

The temperature influence on all heat consumes for the process stages are represented in Fig. 11.

The increment in the reaction temperature produces higher needs on the heating stage (Qc) to expense of obtaining improvements in the final H_2 yield. In the reforming stage (Qr), this effect is similar although less drastic, because the exothermic reactions (RWGS and coal formation) occurring at those high temperatures compensate the system energetically. As was discussed, the temperature favors the final yield and selectivity of H_2 (see Figs. 4 and 6), also the selectivity to monoxide increases slightly when the temperature overcomes the 823 K because of the reversible water gas reaction (RWGSR), however, the hydrogen levels obtained justify the work at this high temperatures. The levels of CO produced (CO <5%mol) are easily assimilable for the SOFC fuel cell working at high temperatures (873 K). Moreover, when temperature rises the second heating stage (Qa: between reforming and fuel cell) is less important, because the difference between the syngas temperature and the fuel cell operating conditions ($T = 823$K) are very slight.

The fuel cell efficiency and the fuel utilization are favored by the temperature adjustment, although when the 823 K are surpassed the level of use of the fuel ($1 - \mathrm{LHV_{in}}/\mathrm{LHV_{out}}$) falls due to the in situ WGSR, which stops to contribute in H_2 and begins to take place in inverse sense (RWGS), this is a constraint of the model because the problem of the fuel cell reaction is rather complex and needs the use of a more complex mathematical analysis as CFD.

8. Conclusions

This paper has allowed proposing a pseudo-homogeneous model useful to design a steam reformer prototype that exhibit very good performance parameters (S_H, Y_H, X_E) at specific temperature and R_{AE}, respectively.

Also a novel kinetic model was proven to describe the experimental data. This was a Lagmuir-Hishelwood model.

Also the heat consumption in all process steps was quantified being established the strong influence that R_{AE} has on vaporization and heating stages, while the increment in the reaction temperature reduces the needs on heat at conditioning stage.

Finally, it can be concluded that high temperatures (above 773 K) and water/ethanol ratios (about 4.5–5) promote on Ni/Al_2O_3 catalyst, the reforming efficiency and the hydrogen yield (4.1) and selectivity (91%).

Acknowledgments

The authors wish to acknowledge to editor and unknown referees. Arteaga acknowledges the researchers of the Catalytic Productions Laboratory of Universidad de Buenos Aires and the CYTED (Project IV-21).

References

[1] S.D. Minteer, Alcoholic fuels: an overview, in: Sect. Application of Alcoholic fuels, Taylor and Francis Group, 2007.
[2] J. Sun, X.P. Qiu, F. Wu, W.T. Zhu, H_2 from steam reforming of ethanol at low temperature over Ni/Y_2O_3, Ni/La_2O_3 and Ni/Al_2O_3 catalysts for fuel-cell, Int. J. Hydrogen Energy 30 (2005) 437–445.
[3] J.H. Hirschenhofer, D.B. Stauffer, R.R. Engleman, M.G. Klett, Fuel Cells Handbook, sixth ed., EG and G Technical Services, Inc. Science Applications International Corporation, National Energy Technology Laboratory, P.O. Box 880, Morgantown, West Virginia 26507-0880.
[4] J. Comas, F. Marino, M. Laborde, N. Amadeo, Bio-ethanol steam reforming on Ni/Al_2O_3 catalyst, Chem. Eng. J. 98 (2004) 61–68.
[5] M.A. Laborde, E.Y. Garcia, Hydrogen production by steam reforming of ethanol: thermodynamic analysis, Int. J. Hydrogen Energy 16 (1991) 307.
[6] K. Vasudeva, N. Mitra, P. Umasankar, S.C. Dhingra, Steam reforming of ethanol for hydrogen production: thermodynamic analysis, Int. J. Hydrogen Energy 21 (1996) 13–18.
[7] V. Fierro, O. Akdim, H. Provendier, C. Mirodatos, Ethanol oxidative steam reforming over Ni-based catalysts, J. Power Sources 145 (2005) 659–666.
[8] V. Fierro, V. Klouz, O. Akdim, C. Mirodatos, Oxidative reforming of biomass derived ethanol for hydrogen production in fuel cell applications, Catal. Today 75 (2005) 141–144.
[9] F. Marino, M. Boveri, G. Baronetti, M.A. Laborde, Hydrogen production from steam reforming of bioethanol using $Cu/Ni/K/g\text{-}Al_2O_3$ catalysts. Effect of Ni, Int. J. Hydrogen Energy 26 (2001) 665–668.
[10] F. Marino, M. Boveri, G. Baronetti, M. Laborde, Hydrogen production via catalytic gasification of ethanol. A mechanism proposal over copper-nickel catalysts, Int. J. Hydrogen Energy 29 (2004) 67–71.
[11] A. Therdthianwong, T. Sakulkoakiet, S. Therdthianwong, Hydrogen production by catalytic ethanol steam reforming, Sci. Asia 27 (2001) 193–198.
[12] A. Akande, A. Aboudheir, R. Idem, A. Dalai, Kinetic modeling of hydrogen production by the catalytic reforming of crude ethanol over a co-precipitated $Ni\text{-}Al_2O_3$ catalyst in a packed bed tubular reactor, Int. J. Hydrogen Energy 31 (2006) 1707–1715.
[13] V. Klouz, V. Fierro, P. Denton, H. Katz, J.P. Lisse, S. Bouvot-Mauduit, C. Mirodatos, Ethanol reforming for hydrogen production in a hybrid electric vehicle: process optimization, J. Power Sources 105 (2002) 26–34.
[14] J.M. Smith, Ingeniería de la Cinética Química, sixth ed., Mc Graw Hill Co., 1991, ISBN-0-07-058710-8.
[15] S.M. Walas, Chemical Process Equipment Selection and Design, Butterworth-Heinemann Series in Chemical Engineering, 1990, ISBN 0-7506-9385-1.
[16] R.H. Perry, D.W. Green, Chemical Engineers Handbook, McGraw-Hill Companies Inc., 1999.
[17] M.S. Peters, K.D. Timmerahus, R.E. West, Plant Design and Economics for Chemical Engineers, fifth ed., McGraw Hill Companies Inc. Chemical Engineering Series, 2003.
[18] N.P. Brandon, D. Corcoran, D. Cummins, et al., Development of metal supported solid oxide fuel cells for operation at 500–600 °C, J. Mater. Eng. Perform. 13–3 (2004) 253–256.
[19] Y. Casas, M. Morales, L.E. Arteaga, Estudio de alternativas tecnológicas de reformación de bioetanol como fuente de energía renovable, Rev. Cub. Química XVIII (1) (2006) 140–146, ISSN: 0258-5995.
[20] C. Diagne, H. Idriss, K. Pearson, M. Gómez, A. Kiennemann, Efficient hydrogen production by ethanol reforming over Rh catalysts. Effect of addition of Zr on CeO_2 for the oxidation of CO to CO_2, C. R. Chim. 7 (2004) 61–622.